

Modeling adsorption kinetics of trichloroethylene onto biochars derived from soybean stover and peanut shell wastes

Mahtab Ahmad · Sang Soo Lee · Sang-Eun Oh ·
Dinesh Mohan · Deok Hyun Moon · Young Han Lee ·
Yong Sik Ok

Received: 23 December 2012 / Accepted: 22 March 2013 / Published online: 23 April 2013
© Springer-Verlag Berlin Heidelberg 2013

Abstract Trichloroethylene (TCE) is one of the most hazardous organic pollutants in groundwater. Biochar produced from agricultural waste materials could serve as a novel carbonaceous adsorbent for removing organic contaminants from aqueous media. Biochars derived from pyrolysis of soybean stover at 300 °C and 700 °C (S-300 and S-700, respectively), and peanut shells at 300 °C and 700 °C (P-300 and P-700, respectively) were utilized as carbonaceous adsorbents to study batch aqueous TCE remediation kinetics. Different rate-based and diffusion-based kinetic models were adopted to understand the TCE adsorption mechanism on biochars. With an equilibrium time of 8–10 h, up to 69 % TCE was removed from water. Biochars produced at 700 °C were more effective than those produced at 300 °C. The P-700 and S-700 had lower molar H/C and O/C versus P-300 and S-300 resulting in high aromaticity and low polarity accompanying with high surface area and high adsorption capacity. The pseudo-second order and intraparticle diffusion models were well fitted to the kinetic data, thereby,

indicating that chemisorption and pore diffusion were the dominating mechanisms of TCE adsorption onto biochars.

Keywords Black carbon · Charcoal · Crop residue · Proximate analysis · Slow pyrolysis · Sorption dynamics

Introduction

Release of chlorinated hydrocarbons is continually threatening the groundwater environment (Yang et al. 2011). Trichloroethylene (TCE) is a dense non-aqueous phase liquid, which is water soluble substance having 1.1 kg m⁻³ solubility at 25 °C (Wei and Seo 2010). Because of high density (1,460 kg m⁻³), TCE spills are not easily washable and can percolate down causing severe groundwater contamination (Jo et al. 2010). Therefore, TCE is considered as one of the dangerous and toxic organic contaminants in the groundwater emanating from industries (Erto et al. 2010). The groundwater contamination by TCE has been extensively reported worldwide (Klasson et al. 2009; Wei and Seo 2010). In Korea, TCE is one of the frequently occurring organic contaminants in groundwater nearby industrial and urban areas (Lee and Lee 2004). The groundwater of an industrial complex at Wonju-si has been reported to be contaminated with TCE (Baek and Lee 2011). Approximately 300,000 m² of this complex is contaminated with TCE (Yu et al. 2006). Up to 1.52 mg L⁻¹ TCE, which is 51 times higher than the prescribed Korean standard limit of 0.03 mg L⁻¹, was reported in this area (Yu et al. 2006). Multiple industrial facilities including an asphalt testing laboratory and a molding company have been identified as the major sources of the TCE groundwater contamination (Baek and Lee 2011).

Numerous technologies such as air-stripping, reactive barriers, adsorption, thermal desorption, and biodegradation have

Responsible editor: Philippe Garrigues

M. Ahmad · S. S. Lee · S.-E. Oh · Y. S. Ok (✉)
Korea Biochar Research Center & Department of Biological
Environment, Kangwon National University, Chuncheon 200-701,
South Korea
e-mail: soilok@kangwon.ac.kr

D. Mohan
School of Environmental Sciences, Jawaharlal Nehru University,
New Delhi 110067, India

D. H. Moon
Department of Environmental Engineering, Chosun University,
Gwangju 501-759, South Korea

Y. H. Lee
Division of Plant Environmental Research, Gyeongsangnam-do
Agricultural Research and Extension Service, Jinju 660-360,
South Korea

been proposed for TCE remediation from contaminated groundwater (Chung et al. 2004; Yang et al. 2007; Klasson et al. 2009; Kim et al. 2012). Among these, adsorption is one of the most certain remediation techniques used to purify TCE contaminated groundwater (Leboda et al. 1997). Carbon materials such as activated carbon (AC)/charcoal, graphitized carbon black, carbon molecular sieves, and carbon nanotubes are most frequently used as effective adsorbents (Leboda et al. 1997; Ahmad et al. 2012a; Alberti et al. 2012). However, the adsorption capacities of these materials are highly dependent on their micro-porous structures and the presence of surface functional groups. Another common consideration to use these carbonaceous adsorbents is the relatively high cost. Many of these adsorbents are derived from wood and coal, and it led to an increase of the application cost. Therefore, various raw materials or wastes, including eggshells, oyster shells, mussel shells, corals, olive stones, coconut husk, and agricultural waste materials, have been used as low cost environment-friendly adsorbents for water remediation (Ioannou and Simitzis 2009; Ok et al. 2011; Park et al. 2011; Ahmad et al. 2012b, c). These materials are either used as a raw form or after physicochemical modifications to enhance their adsorption efficiencies (Ok et al. 2010; Ahmad et al. 2012d; Lee et al. 2013; Pelleria et al. 2012). Thermal modification of biomass via pyrolysis and carbonization is gaining much popularity. The biomass-derived black carbon also known as “biochar” is being newly employed to soil for carbon sequestration and soil fertility (Uchimiya et al. 2010; Yu et al. 2010; Awad et al. 2012). Biochar has also been applied to remediate contaminants in water and wastewater (Xu et al. 2012). The use of biochar as an adsorbent is very economical compared to AC (Qui et al. 2009).

Biomass types, pyrolysis and/or carbonization temperature, residence time, and heat transfer rate determine the structural and chemical properties of biochar. Pyrolysis processes induce the pore development in biochar by evaporation of gases, thereby expanding their surface area (Novak et al. 2009). Consequently, the carbon fractions in biochars can be categorized into polyaromatic, elemental, or graphitic structures (Chun et al. 2004). These transitional phase changes would strongly influence biochar function as a carbonaceous adsorbent (Keiluweit et al. 2010). Additionally, biochar efficiency as an adsorbent depends on surface area related to physical and chemical adsorption on the active sites of biochar (Ioannou and Simitzis 2009).

Adsorption kinetics generally describes the time-dependent uptake of an adsorbate by an adsorbent in an aqueous or gaseous phase. Thus, the application of adsorption kinetics is useful in determining the adsorption mechanism. Earlier we have reported the TCE adsorption equilibrium studies on biochars (Ahmad et al. 2012e). In the present investigation, TCE sorption dynamics on biochars derived from soybean stover and peanut shells pyrolyzed at 300 °C and 700 °C are

reported. Various rate and diffusion models were used to establish the possible sorption mechanism.

Materials and methods

Biochars development as adsorbents

Soybean stover and peanut shells were converted into biochars. A detailed description of biochar production and characterization is available elsewhere (Ahmad et al. 2012e). Briefly, soybean stover and peanut shells waste materials were pyrolyzed in a muffle furnace (MF 21 GS, Jeio Tech, Korea) in absence of air. Pyrolysis was carried out at 300 °C and 700 °C with an increment rate of 7 °C per min. The peak temperature of 300 °C or 700 °C was maintained for 3 h to complete the carbonization. The pyrolyzed products were allowed to cool down in the furnace and stored in an air-tight container. Biochars thus produced from soybean stover and peanut shells at 300 °C and 700 °C were designated as S-300, S-700, P-300, and P-700, respectively. A commercially available biochar produced from oak wood (OW) at 400 °C was obtained from Gangwon Charmsoot Company located in Hoengseong-gun, Gangwon province, Korea. A powdered AC was also purchased from Sigma Aldrich Company to compare the results from other adsorbents. All adsorbents used in this study were characterized before adsorption experiment. Structural characteristics of the adsorbents were determined by measuring specific surface area, pore volume, and pore diameter by an adsorption apparatus (Micromeritics, ASAP 2010 v 5.02H, USA). The elemental composition of C, H, and O was determined by an elemental analyzer (Flash EA 1112 series, CE Instruments, UK), and then molar H/C and O/C ratios were calculated from the elemental analysis results.

Adsorption kinetics experiment

Batch adsorption kinetics experiments were conducted with different biochars and AC to determine the TCE adsorption (Yang et al. 2006). Reagent grade TCE (99 % purity) was purchased from Wako Pure Chemical Industries (Osaka, Japan). The sorbate solution (50 mg L⁻¹) was prepared by dissolving TCE in ultrapure water obtained from a water purification system (Arium® Pro UV/DI, Sartorius Stedium Biotech, Germany). The water was buffered to pH 7 using 1 mM phosphate buffer (0.5 mM Na₂HPO₄·H₂O and 0.5 mM NaH₂PO₄) to reduce the effect of adsorbents on solution pH (Quinlivan et al. 2005). The carbonaceous adsorbents were added to the TCE solution at a rate of 1.0 g L⁻¹ in Teflon-lined screw capped glass vials. The vials were fully filled without headspace to minimize TCE volatilization loss, and placed on a horizontal shaker set to

50 rpm and 25 °C. Three replicates for each adsorbent and control (without adsorbent) were performed. At specific time intervals of 0.25, 0.5, 0.75, 1.0, 1.5, 2.0, 2.5, 3.0, 4.0, 5.0, 6.0, 8.0, 10.0, 12.0, 16.0, 20.0, 24.0, 32.0, 40.0, and 48.0 h, three vials of each treatment were removed. An aliquot of the solution was filtered through a 0.45- μm pore-size syringe-filter and transferred to a 2-mL amber-colored-glass-vial for TCE analysis. Aqueous phase concentrations of TCE were measured at specific time intervals (t), while the uptake of TCE at time t (q_t in mg g^{-1}) was calculated using Eq. (1) (Ok et al. 2007; Salih et al. 2011):

$$q_t = [(C_0 - C_t)v]/m \quad (1)$$

where C_0 and C_t are the TCE initial and equilibrium concentrations (in mg L^{-1}) at time t , v is the solution volume (in L), and m is the adsorbent dose (in g).

Kinetic models

Various kinetic models were used to investigate the sorption mechanism of TCE adsorption on carbonaceous adsorbents. The linear form of first order kinetic equation can be expressed as (Almaroai et al. 2012):

$$\ln q_t = \ln q_0 - k_1 t \quad (2)$$

where q_t and q_0 are the amounts of TCE adsorbed at time t and 0 min, while k_1 is the rate constant for the first order reaction.

The linear form of second order kinetics is (Almaroai et al. 2012):

$$1/q_t = 1/q_0 - k_2 t \quad (3)$$

where k_2 is the second order rate constant.

The pseudo-first order equation is generally expressed as (Wong et al. 2004):

$$\ln(q_e - q_t) = \ln q_e - k_1' t \quad (4)$$

where q_e is the sorption capacity at equilibrium (in mg g^{-1}) and k_1' is the rate constant for a pseudo-first order reaction.

The pseudo-second order kinetics equation is expressed as (Plazinski et al. 2009):

$$t/q_t = 1/k_2' q_e^2 + (1/q_e)t. \quad (5)$$

where k_2' is the rate constant for a pseudo-second order reaction. Initial sorption rate (h , in $\text{mg g}^{-1} \text{min}^{-1}$) can be calculated from the intercept of Eq. (5).

The Elovich equation can be expressed as (Almaroai et al. 2012):

$$q_t = 1/\beta \ln(\alpha\beta) + (1/\beta) \ln t \quad (6)$$

where α is the initial sorption rate (in $\text{mg g}^{-1} \text{min}^{-1}$) and β is the sorption constant.

The power function equation can also be used to describe the adsorption kinetics as follows (Almaroai et al. 2012):

$$\ln q_t = \ln b + k_f (\ln t) \quad (7)$$

where k_f is the rate coefficient value (in $\text{mg g}^{-1} \text{min}^{-1}$) and b is the rate constant.

The intraparticle diffusion model equation can be expressed as (Almaroai et al. 2012):

$$q_t = c + k_{id} t^{0.5} \quad (8)$$

where k_{id} is the apparent diffusion rate constant (in $[\text{mg g}^{-1}]^{0.5}$) and c is the diffusion constant.

The goodness of fit for the models was evaluated by comparing the coefficient of determination (r^2) and standard error of estimates (SEE) values. The SEE values were calculated using Eq. (9) (Mohammad and Maya 2011):

$$SEE = \sqrt{(\Sigma q_{\text{exp}} - \Sigma q_{\text{calc}})^2 / (n - 2)} \quad (9)$$

where q_{exp} and q_{calc} are the experimental and model calculated sorption capacities (in mg g^{-1}), and n is the number of observations.

Analytical methods

Biochars and AC were characterized for various structural and elemental characteristics, and details were reported elsewhere (Ahmad et al. 2012e). In summary, the traditional N_2 gas adsorption technique was used to determine the surface area using a gas sorption analyzer (NOVA-1200, Quantachrome Corp., USA). The isotherms were obtained by plotting the N_2 adsorbed per gram of sample versus the relative vapor pressure (P/P_0) of N_2 ranging from 0.02 to 0.2. The surface area was calculated by fitting the data to the Brunauer–Emmett–Teller (BET) equation, and total pore volume was estimated from N_2 adsorption at $P/P_0 \sim 0.5$ (Park and Komarneni 1998). Surface morphological microstructures of the carbonaceous adsorbents were determined using a field emission scanning electron microscope (FE-SEM) equipped with energy dispersive spectroscopy (SU8000, Hitachi, Japan). SEM images were obtained from a 50- μm area of sample placed on a double-sided platinum coated tape. An elemental analyzer (EA1110, CE Instruments, Italy) was used to determine the elemental composition (C, H, N, S, and O) of adsorbents. The sample was combusted at 1,014 °C and electrical output signals proportional to the amount of eluted gas were generated by a thermo conductivity detector (TCD).

A high performance liquid chromatograph (HPLC, SCL-10A, Shimadzu, Japan) equipped with an auto-sampler (SIL-10AD, Shimadzu, Japan) and UV-VIS detector (SPD-10A, Shimadzu, Japan) was used to analyze the aqueous TCE concentration. A reverse-phase Sunfire C18 column

(Waters, USA; 4.6 mm×250 mm) was employed in a column oven (CTO-10AS, Shimadzu, Japan). The mobile phase was a mixture of 85:15 v/v acetonitrile and water. The eluent was pumped isocratically at the rate of 1.0 mL min⁻¹. A 10-μL aliquot of the sample solution was injected onto the column heated at 40 °C and the absorbance was measured at 214 nm.

Statistical analysis

Mean values of three replicates from each batch experiment were used as input into the kinetic models to calculate various model parameters. Linear regression fittings were employed.

Results and discussion

Properties of carbonaceous adsorbents

Table 1 shows the physicochemical properties of AC, OW, and developed biochars (i.e., S-300, P-300, S-700, and P-700). Relatively high surface area was obtained for S-700 (420.33 m² g⁻¹) and P-700 (448.23 m² g⁻¹) versus S-300 (5.61 m² g⁻¹) and P-300 (3.14 m² g⁻¹), showing the pyrolysis temperature effect. Generally, the increased surface area at high pyrolysis temperature is related to the development of micropores in biochars due to the removal of volatile materials (Lee et al. 2010). Biochars produced at 700 °C are characterized by the pore volume of 0.19 and 0.20 cm³ g⁻¹ for S-700 and P-700, respectively. The pore diameters were 1.09 and 1.12 nm for S-700 and P-700 biochars, respectively. Furthermore, the micropores development in S-700 and P-700 is also apparent in their SEM images (Fig. 1). The highest surface area of 1,110 m² g⁻¹ accounted for AC may be due to the additional activation processes generally applied after feedstock carbonization during the AC synthesis. The OW biochar had a medium range surface area of 270.76 m² g⁻¹, resulting from its pyrolysis at 400 °C.

Total C, H, and O contents in all adsorbents ranged from 68.27–90.85 %, 0.90–4.29 %, and 8.24–25.89 %, respectively. The total C contents were higher in S-700 (81.98 %) and P-700 (83.76 %) as compared to S-300 (68.81 %) and P-300 (68.27 %), indicating a higher degree of carbonization at a higher temperature. Contrarily, the H and O contents were lower in S-700 (1.27 % and 15.45 %, respectively) and P-700 (1.75 % and 13.34 %, respectively) than S-300 (4.29 % and 24.99 %) and P-300 (3.85 % and 25.89 %, respectively). Removal of O at high pyrolysis temperature may result in increasing hydrophobicity or decreasing polarity. Li et al. (2002) reported that the removal of O at high pyrolysis temperature makes the carbon surface more basic due to the acidic functional groups removal, thereby, inducing these carbons less polar. The molar ratios of H/C and O/C were calculated as indicators of aromaticity and polarity of the biochars and AC, respectively (Uchimiya et al. 2010). Lower ratios of H/C and O/C in S-700 (0.19 and 0.14, respectively), P-700 (0.25 and 0.12, respectively), OW (0.16 and 0.08, respectively), and AC (0.12 and 0.07, respectively) than S-300 and P300 indicated high aromaticity and low polarity. Chun et al. (2004) has reported increase in aromaticity and decrease in polarity at high pyrolysis temperatures in the chars derived from wheat residues. The structural characteristics and elemental compositions of biochars revealed that the pyrolysis temperature had a strong influence on biochar properties. Moreover, surface area and total C contents of the biochars increased with rise in pyrolysis temperature during feedstock combustion. Removal of O and H at high temperature resulted in biochars having high aromaticity and low polarity. These results imply that the specific properties of biochars may influence their adsorptive behavior towards organic contaminants remediation including TCE.

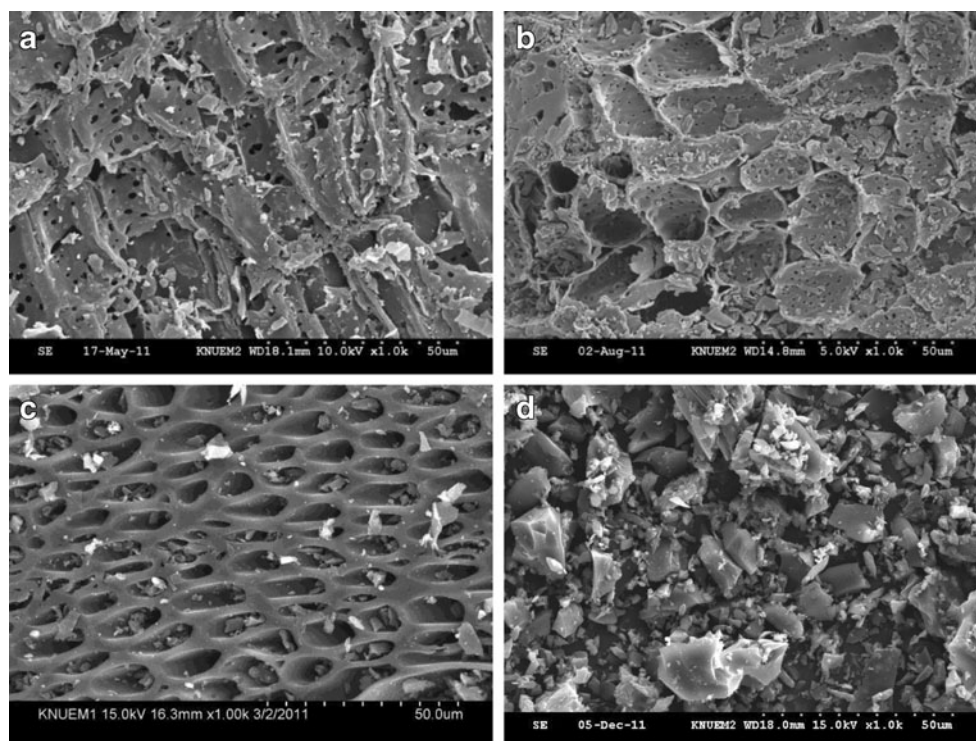
TCE sorption dynamics

TCE sorption dynamics on various biochars with time are shown in Fig. 2. Rapid TCE adsorption was observed within

Table 1 Selected physicochemical properties of biochars derived from soybean stover (S-300 and S-700) and peanut shells (P-300 and P-700), commercial oak biochar (OW), and activated carbon (AC) (Extended result of Ahmad et al. (2012e))

Sample	S-300	S-700	P-300	P-700	OW	AC
Structural characteristics						
Surface area (m ² g ⁻¹)	5.61	420.33	3.14	448.23	270.76	1110
Pore volume (cm ³ g ⁻¹)	–	0.19	–	0.20	0.12	0.64
Pore diameter (nm)	–	1.09	–	1.12	1.10	1.44
Elemental composition (wt%)						
C	68.81	81.98	68.27	83.76	88.71	90.85
H	4.29	1.27	3.85	1.75	1.21	0.90
O	24.99	15.45	25.89	13.34	9.72	8.24
Molar H/C	0.74	0.19	0.67	0.25	0.16	0.12
Molar O/C	0.27	0.14	0.29	0.12	0.08	0.07

Fig. 1 Scanning electron micrographs of **a** biochar derived from soybean stover at 700 °C, S-700, **b** biochar derived from peanut shell at 700 °C, P-700, **c** commercial oak biochar, OW, and **d** activated carbon, AC



1 h of contact time. Specifically, S-300, S-700, P-300, and P-700 removed 39 %, 43 %, 36 %, and 51 % TCE, respectively. This was followed by a slow removal phase resulting in 48 %, 60 %, 50 %, and 68 % maximum TCE removal, respectively, after 8 h of contact time. In the case of AC, rapid adsorption occurred within 0.25 h of contact time, removing 81 % TCE, followed by a short slow phase of 1.5 h, causing a maximum 87 % TCE removal. However, the application of OW followed only the slow phase TCE adsorption completing in 20 h with a maximum removal of

46 %. The general two-phase adsorption, consisting predominantly of a rapid phase and a relatively slow phase, is a commonly observed phenomenon (Saeed et al. 2005; Pelleria et al. 2012), and can be explained by the abundant availability of active sites in biochars, which then become progressively saturated with time. The equilibrium time for S-300, S-700, P-300, and P-700 was 8–10 h, whereas OW required 20–24 h. On the other hand, the equilibrium time for AC was only 1.5–2 h. At equilibrium, the maximum TCE adsorption by various biochars followed the order: P-700>S-700>P-300>OW≥S-300. However, AC showed high adsorption of TCE (43.52 mg g^{-1}) than biochars at equilibrium, which may be attributed to its high surface area ($1,110 \text{ m}^2 \text{ g}^{-1}$).

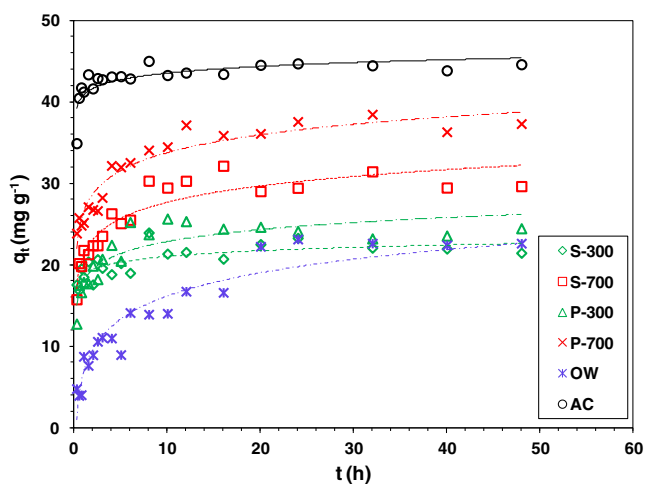


Fig. 2 TCE adsorption kinetics on biochars derived from soybean stover (S-300 and S-700) and peanut shells (P-300 and P-700), commercial oak biochar (OW) and activated carbon (AC). (Initial TCE concentration, 50 mg L^{-1} ; adsorbent dose, 1 g L^{-1})

It is noteworthy that the biochars produced at 700 °C were more effective in TCE adsorption than those produced at 300 °C, thereby, indicating the temperature effect on their adsorption capacities. Pyrolysis temperature significantly affected the structural and elemental properties of biochars (Table 1). Specifically, the greater increases of the surface area for S-700 ($420.33 \text{ m}^2 \text{ g}^{-1}$) and P-700 ($448.23 \text{ m}^2 \text{ g}^{-1}$) compared to S-300 ($5.61 \text{ m}^2 \text{ g}^{-1}$) and P-300 ($3.14 \text{ m}^2 \text{ g}^{-1}$), resulting from high pyrolysis temperature, enhanced their TCE adsorption efficiency. TCE adsorption on OW (22.65 mg g^{-1}) was surprisingly low, in spite of its high surface area ($270.8 \text{ m}^2 \text{ g}^{-1}$) versus S-300 and P-300. This may be due to the competitive effect of TCE with acetate in the OW (Erto et al. 2010) because wood vinegar (acetic acid) is being produced as a by-product of OW manufacture. Erto et al. (2010) emphasized that TCE adsorption capacity

onto carbonaceous adsorbents is greatly lowered by the presence of ethyl acetate because of its competitive effect with TCE. Recently, Spokas et al. (2011) qualitatively analyzed volatile organic compounds in a variety of biochars, and reported the presence of 52 % methyl acetate content in the wood biochars. Sorption of volatile organic compounds such as acetates produced during pyrolysis or from direct contact with liquor (vinegar) onto the OW may cause the active sites to be occupied, consequently resulting in lowering the TCE adsorption compared to other biochars.

Adsorption mechanism

Sorption process is mainly controlled by the sorbate to sorbent transport, film diffusion through the boundary layer, intraparticle diffusion of ions or molecules, and chemisorption (Alberti et al. 2012). The greatest confrontation offered by one of these stages becomes the rate-limiting step of the sorption process (Alberti et al. 2012). Kinetic studies were performed to investigate the chemical reaction rates and sorption mechanisms for biochars and AC, having heterogeneous reactive sites. To investigate the sorption mechanism, the experimental data were fitted to various kinetic models listed in Table 2 and discussed under kinetic model.

The models were evaluated based on r^2 and *SEE* values as given in Table 3. The r^2 value is the most reliable and widely used error function to determine the best fit kinetic model (Kumar et al. 2008). According to the r^2 values, kinetic data had a good fit with a pseudo-second order model followed by the intraparticle diffusion model for all adsorbents (Fig. 3). The kinetic parameters obtained from various models are summarized in Table 4.

The pseudo-second order kinetic model has been successfully applied and the rate constant (k_2'), the adsorption capacity (q_e), and the initial adsorption rate (h) were determined simultaneously (Ho and Ofomaja 2006). The rate

constant is a time-scaling factor in determining the time required to reach an equilibrium-state. High rate constant indicates a short time and vice versa (Plazinski et al. 2009). The k_2' values obtained from pseudo-second order model for different adsorbents ranged from 0.250×10^{-3} to $5.409 \times 10^{-3} \text{ g mg}^{-1} \text{ min}^{-1}$. The k_2' values follow the order: AC>S-300>P-300>S-700>P-700>OW. The high k_2' values obtained for AC, S-300, and P-300 indicated the enhanced mobility of TCE, which reached the solid surfaces in a short time interval. This finding agrees with the corresponding h values of the adsorbents, suggesting a high initial sorption rate. The q_e values calculated from the kinetic model ranged from 21.38 to 45.01 mg g^{-1} for different adsorbents. This follows the order: AC>P-700>S-700>P-300>S-300>OW. The high q_e values for P-700 (37.00 mg g^{-1}) and S-700 (29.38 mg g^{-1}) could be attributed to their surface area imparted at high pyrolysis temperature versus P-300 (24.30 mg g^{-1}) and S-300 (21.94 mg g^{-1}). The positive linear relationship between surface area and equilibrium sorption capacities ($r^2=0.877$) is shown in Fig. 4. Maximum capacity of equilibrium sorption (45.01 mg g^{-1}) was obtained for AC due to its higher surface area than other biochars. The best fit of adsorption kinetics data was obtained with the pseudo-second order model suggesting the chemisorption to be the rate-limiting step, i.e., the rate of direct adsorption controls the overall sorption kinetics for all carbonaceous adsorbents (Plazinski et al. 2009). These findings are in agreement with the results published recently for the Cu(II) adsorption on biochars (Pellera et al. 2012).

In the kinetics analysis, TCE sorption on carbonaceous adsorbents may also involve intraparticle diffusion through macro- (>50 nm), meso- (2–50 nm), and micro- (<2 nm) pores, which could be the rate-determining step of the sorption process. Among diffusion-driven kinetics, the intraparticle diffusion model had a good fit (relatively high r^2 values) with the experimental data. The intraparticle diffusion rate constant

Table 2 Kinetic models and their mathematical expressions used to fit the data

Model	Mathematical expression	Plot	Parameters
First order	$\ln q_t = \ln q_0 - k_1 t$	$\ln q_t$ vs t	k_1 = slope
Second order	$1/q_t = 1/q_0 - k_2 t$	$1/q_t$ vs t	k_2 = slope
Pseudo-first order	$\ln (q_e - q_t) = \ln q_e - k_1' t$	$\ln (q_e - q_t)$ vs t	k_1' = slope q_e = intercept
Pseudo-second order	$t/q_t = 1/k_2' q_e^2 + (1/q_e) t$	t/q_t vs t	k_2' = slope ² /intercept q_e = 1/slope h = 1/intercept
Elovich	$q_t = 1/\beta \ln (\alpha\beta) + (1/\beta) \ln t$	q_t vs $\ln t$	a = slope β = intercept
Power function	$\ln q_t = \ln b + k_f (\ln t)$	$\ln q_t$ vs $\ln t$	k_f = slope b = intercept
Intraparticle diffusion	$q_t = c + k_{id} t^{0.5}$	q_t vs $t^{0.5}$	k_{id} = slope c = intercept

Table 3 Coefficients of determination (r^2) and standard errors of estimate (SEE) for kinetic models used to model TCE kinetic data onto biochars derived from soybean stover (S-300 and S-700) and peanut shells (P-300 and P-700), commercial oak biochar (OW), and activated carbon (AC)

Adsorbent	First order		Second order		Pseudo-first order		Pseudo-second order		Elovich		Power function		Intraparticle diffusion	
	r^2	SEE	r^2	SEE	r^2	SEE	r^2	SEE	r^2	SEE	r^2	SEE	r^2	SEE
S-300	0.485	0.070	0.478	0.004	0.481	0.202	0.985	1.078	0.464	1.430	0.478	0.071	0.495	1.388
S-700	0.788	0.080	0.705	0.004	0.816	0.076	0.982	0.711	0.878	1.355	0.899	0.055	0.892	1.279
P-300	0.726	0.098	0.647	0.006	0.679	0.130	0.974	0.820	0.816	1.381	0.834	0.077	0.819	1.466
P-700	0.894	0.049	0.868	0.002	0.963	0.058	0.993	0.520	0.861	1.518	0.881	0.051	0.948	1.007
OW	0.674	0.303	0.463	0.051	0.763	0.194	0.916	5.225	0.856	1.977	0.874	0.207	0.908	1.581
AC	0.676	0.055	0.655	0.002	0.894	0.219	0.999	0.023	0.877	1.300	0.866	0.035	0.794	1.687

(k_{id}) was relatively high for AC ($1.339 \text{ mg g}^{-1} \text{ min}^{-0.5}$), S-700 ($0.618 \text{ mg g}^{-1} \text{ min}^{-0.5}$), P-700 ($0.575 \text{ mg g}^{-1} \text{ min}^{-0.5}$), and P-300 ($0.599 \text{ mg g}^{-1} \text{ min}^{-0.5}$), showing high adsorption rates.

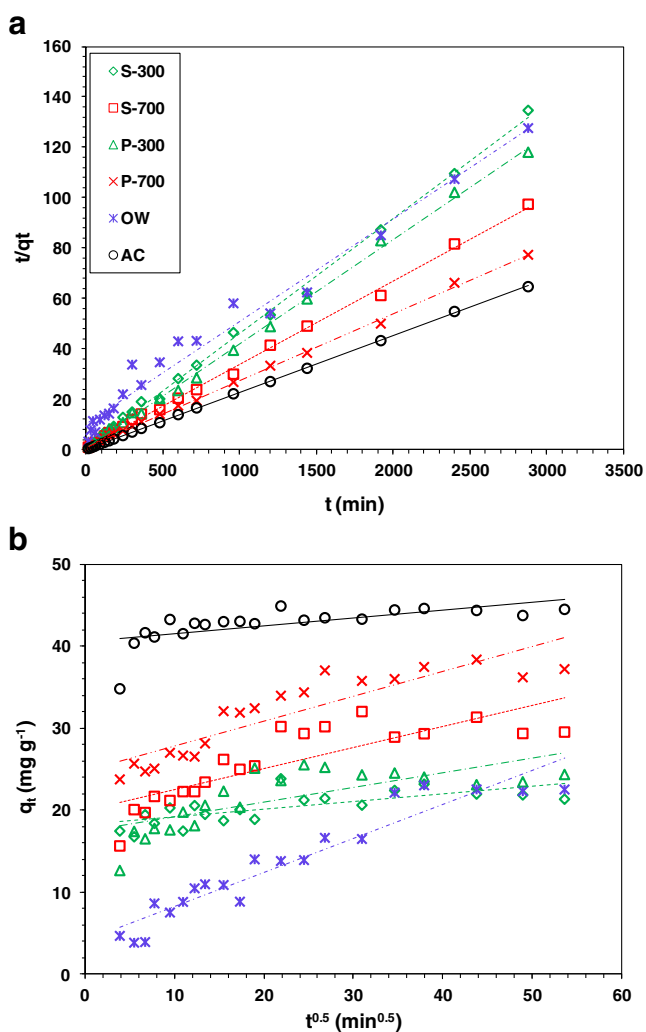


Fig. 3 Linear regression fittings of **a** pseudo-second order and **b** intraparticle diffusion models for TCE adsorption kinetics on biochars derived from soybean stover (S-300 and S-700) and peanut shells (P-300 and P-700), commercial biochar (OW) and activated carbon (AC)

The boundary layer thickness (c) ranged from 2.65 to 31.37. Regarding the boundary layer effect, the low c values for OW (2.65) indicated less resistance to mass transfer, thus causing an increase in the mobility of TCE towards carbonaceous adsorbent (Kannan and Sundaram 2001; Hameed and El-Khaiary 2008). The macro- and meso-porous structures of the adsorbents (Fig. 1), especially in the cases of OW, S-700, and P-700 biochars, may have resulted in greater diffusion of TCE within adsorbent particles. In the batch type kinetics experiment, the intraparticle diffusion has been reported to be the rate-limiting step by El-Ashtoukhy et al. (2008).

The relation between adsorbate mass per unit adsorbent mass can also be described by the power function equation (Witek-Krowiak et al. 2011). The values of r^2 and SEE calculated in the power function model ranged from 0.834 to 0.899 and 0.035 to 0.207, respectively, for various adsorbents except S-300. The rate coefficient (k_f) values were high for OW ($0.373 \text{ mg g}^{-1} \text{ min}^{-1}$), S-700 ($0.148 \text{ mg g}^{-1} \text{ min}^{-1}$), and P-300 ($0.162 \text{ mg g}^{-1} \text{ min}^{-1}$), indicating an increase in TCE adsorption on these adsorbents with time.

The Elovich kinetic model, which was originally applied to describe the gas adsorption phenomenon, is now widely used to explain the aqueous contaminants sorption by assuming strong heterogeneity of sorbent surface (Plazinski et al. 2009). The experimental data had a good fit with the Elovich model as indicated by r^2 values of 0.816–0.878 except S-300. The initial adsorption rate (α) for various carbonaceous adsorbents was in the order: AC ($4.397 \text{ mg g}^{-1} \text{ min}^{-1}$) > OW ($3.627 \text{ mg g}^{-1} \text{ min}^{-1}$) > P-700 ($3.384 \text{ mg g}^{-1} \text{ min}^{-1}$) > S-700 ($3.269 \text{ mg g}^{-1} \text{ min}^{-1}$) > P-300 ($2.934 \text{ mg g}^{-1} \text{ min}^{-1}$) > S-300 ($1.140 \text{ mg g}^{-1} \text{ min}^{-1}$), indicating relatively high adsorption on biochars produced at 700 °C. This also implies the predominance of TCE chemical sorption on these materials assuming a multilayer sorption, with each layer exhibiting different activation energies for chemisorption (Alberti et al. 2012).

Except for P-700, the first, second, and pseudo-first order rate kinetics could not adequately describe the experimental data as apparent from the r^2 values of <0.8 (Table 3).

Table 4 Parameters obtained from kinetic models used for TCE sorption dynamics modeling onto biochars derived from soybean stover (S-300 and S-700) and peanut shells (P-300 and P-700), commercial oak biochar (OW), and activated carbon (AC)

Adsorbent	First order		Second order		Pseudo-first order		Pseudo-second order			Elovich		Power function		Intraparticle diffusion	
	k_1	k_2	k_1'	q_e	k_2'	q_e	h	α	β	k_f	b	k_{id}	c		
S-300	0.355×10^{-3}	1.788×10^{-5}	1.085×10^{-3}	0.577	2.903×10^{-3}	21.94	1.398	1.140	13.94	0.058	2.684	0.204	16.83		
S-700	1.010×10^{-3}	4.466×10^{-5}	1.331×10^{-3}	1.063	1.141×10^{-3}	29.38	0.985	3.269	6.859	0.148	2.413	0.618	15.40		
P-300	1.323×10^{-3}	7.138×10^{-5}	1.878×10^{-3}	0.960	1.633×10^{-3}	24.30	0.964	2.934	5.487	0.162	2.186	0.599	12.35		
P-700	0.606×10^{-3}	2.036×10^{-5}	1.332×10^{-3}	1.130	0.779×10^{-3}	37.00	1.066	3.384	12.43	0.115	2.794	0.575	21.28		
OW	1.179×10^{-3}	12.73×10^{-5}	0.941×10^{-3}	1.305	0.250×10^{-3}	21.38	0.114	3.627	-7.949	0.373	0.339	0.514	2.65		
AC	2.378×10^{-3}	6.093×10^{-5}	19.12×10^{-3}	1.200	5.409×10^{-3}	45.01	10.96	4.397	24.01	0.113	3.274	1.339	31.37		

Overall, the pseudo-second order, Elovich, and intraparticle diffusion models adequately described the experimental data, thereby, indicating chemisorption and intraparticle diffusion to be the dominant mechanisms in the TCE adsorption on various carbonaceous adsorbents.

Biochar properties and TCE adsorption

The structural characteristics and elemental compositions of biochars influenced TCE removal from water. Particularly in P-700 and S-700, the high surface area and pore volume, and relatively low H/C and O/C molar ratios led to relatively high TCE adsorption. This validated that pyrolysis temperature is a pivotal factor influencing the biochars properties and ultimately affects their adsorption capacities (Chun et al. 2004; Chen et al. 2008). The q_e value calculated from the pseudo-second order kinetics model was plotted as a function of surface area of the carbonaceous adsorbents (Fig. 4). A linear positive correlation indicated that the adsorbents having high surface area had high adsorption capacity for TCE. Furthermore, the lower H/C and O/C molar ratios of P-700, S-700, and AC (Table 1) imparted high aromaticity and low polarity of these materials, resulting in the TCE removal enhancement. The polarity of carbon surfaces is generally decreased by the removal of acidic functional groups at high temperature (Li et al. 2002), minimizing the chance of water cluster formation on the carbon surfaces, thus increasing the sorption of organic contaminants such as TCE (Karanfil and Dastgheib 2004).

The micro-porous structure of biochars (pore size <2 nm) is another important factor controlling TCE adsorption. The TCE diffusion within carbon particles of biochars was also affirmed from a good fit of the experimental data with the intraparticle diffusion model. Another plausible explanation for the relatively high TCE adsorption on P-700, S-700, and AC may be related to their pore diameters (Table 1). Trichloroethylene is a planar molecule having a diameter of 0.56 nm. Thus, it can easily be diffused into the adsorbents pores having a diameter greater than its kinetic diameter. Li et al. (2002) reported that for effective TCE adsorption to take place, a large volume of micropores having ~1.3 to 1.8

times greater diameter than the TCE kinetic diameter are needed in the adsorbents. In the present investigation, P-700 and S-700 were characterized by the pore diameter which is ~2 times greater than TCE kinetic diameter. These findings are in good agreement with findings of Li et al. (2002).

To a lesser extent, feedstock type also influenced the TCE adsorption capacity of biochars. Comparatively, biochars derived from peanut shells were more effective than those derived from soybean stover (Fig. 2). This could probably be due to greater inorganic components in the soybean stover-derived biochars as indicated by higher ash contents (10.41 % to 17.18 %) compared to peanut shell-derived biochars (1.24 % to 8.91 %). Ash minerals can block the organic sorption sites in biochars due to the interaction with inorganic moiety (Zhang et al. 2013).

The efficiency of biochars on TCE adsorption was dependent on surface area, contact time, solute affinity towards adsorbent, number of carbon atoms, and molecular size with respect to adsorbent pore size. The adsorbent properties primarily influenced the TCE removal from water as observed from the analogous behavior of biochars produced at

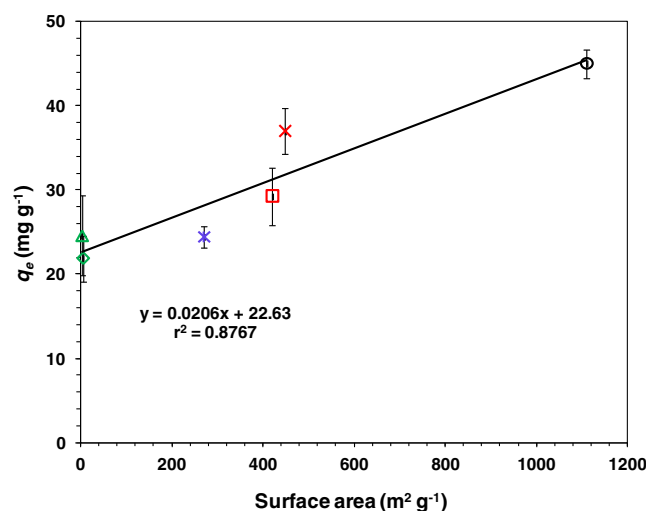


Fig. 4 Correlation between equilibrium sorption capacities of different biochars calculated from pseudo-second order kinetic equation and surface areas

the same pyrolytic temperature. Therefore, a detailed description of adsorbent properties is required to fully utilize the adsorbent capacity in water and wastewater treatment.

Conclusions

In the present investigation, biochars were produced by pyrolyzing soybean stover and peanut shells at 300 °C and 700 °C. The biochars produced at 700 °C were characterized as high surface area, microporosity, aromaticity, and low polarity. High equilibrium sorption capacity was obtained for the biochars produced at a high pyrolysis temperature and commercial AC because of their high surface areas. Furthermore, peanut shell biochar was more effective than biochar produced from soybean stover for TCE adsorption from water. The pseudo-second order and intraparticle diffusion models best fitted the TCE adsorption experimental data obtained for various types of carbonaceous adsorbents. This indicates that chemisorption and pore diffusion were the dominating mechanisms controlling the TCE adsorption. Biochar properties, as affected by the pyrolysis temperature, also influenced their behavior towards TCE adsorption. Overall, biochars derived from agricultural waste materials can be successfully utilized for TCE remediation from water and wastewater, and the specific characteristics of biochar including high surface area, less pore size, high aromaticity and less polarity are recommended for its best performance.

Acknowledgments This study was supported by the Ministry of Environment, Republic of Korea as “The GAIA Project (No. 173-092-010).” Instrumental analysis was supported by the Korea Basic Science Institute, the Environmental Research Institute and the Central Laboratory of Kangwon National University, Korea.

References

- Ahmad M, Lee SS, Yang JE, Ro HM, Lee YH, Ok YS (2012a) Effects of soil dilution and amendments (mussel shell, cow bone, and biochar) on Pb availability and phytotoxicity in military shooting range soil. *Ecotoxicol Environ Saf* 79:225–231
- Ahmad M, Usman ARA, Lee SS, Kim SC, Joo JH, Yang JE, Ok YS (2012b) Eggshell and coral wastes as low cost sorbents for the removal of Pb²⁺, Cd²⁺ and Cu²⁺ from aqueous solutions. *J Ind Eng Chem* 18:198–204
- Ahmad M, Moon DH, Lim KJ, Shope CL, Lee SS, Usman ARA, Kim KR, Park JH, Hur SO, Yang JE, Ok YS (2012c) An assessment of the utilization of waste resources for the immobilization of Pb and Cu in the soil from a Korean military shooting range. *Environ Earth Sci* 67:1023–1031
- Ahmad M, Hashimoto Y, Moon DH, Lee SS, Ok YS (2012d) Immobilization of lead in a Korean military shooting range soil using eggshell waste: an integrated mechanistic approach. *J Hazard Mater* 209–210:392–401
- Ahmad M, Lee SS, Dou X, Mohan D, Sung JK, Yang JE, Ok YS (2012e) Effects of pyrolysis temperature on soybean stover and peanut shell-derived biochar properties and TCE adsorption in water. *Bioresour Technol* 118:536–544
- Alberti G, Amendola V, Pesavento M, Biesuz R (2012) Beyond the synthesis of novel solid phases: Review on modeling of sorption phenomena. *Coord Chem Rev* 256:28–45
- Almaroai YA, Usman ARA, Ahmad M, Kim KR, Vithanage M, Ok YS (2012) Role of chelating agents on release kinetics of metals and their uptake by maize from chromate copper arsenate-contaminated soil. *Environ Technol* 34:747–755
- Awad YM, Blagodatskaya E, Ok YS, Kuzyakov Y (2012) Effects of polyacrylamide, biopolymer and biochar on decomposition of soil organic matter and plant residues determined by ¹⁴C and enzyme activities. *Eur J Soil Biol* 48:1–10
- Baek W, Lee JY (2011) Source apportionment of trichloroethylene in groundwater of the industrial complex in Wonju, Korea: a 15-year dispute and perspective. *Water Environ J* 25:336–344
- Chen B, Zhou D, Zhu L (2008) Transitional adsorption and partition of nonpolar and polar aromatic contaminants by biochars of pine needles with different pyrolytic temperatures. *Environ Sci Technol* 42:5137–5143
- Chun Y, Sheng G, Chiou CT, Xing B (2004) Compositions and sorptive properties of crop residue-derived chars. *Environ Sci Technol* 38:4649–4655
- Chung HH, Choi SW, Ok YS, Jung J (2004) EPR characterization of the catalytic activity of clays for PCE removal by gamma-radiation induced by acid and thermal treatments. *Chemosphere* 57:1383–1387
- El-Ashtoukhy ESZ, Amin NK, Wahab OA (2008) Removal of lead(II) and copper(II) from aqueous solution using pomegranate peel as a new adsorbent. *Desalination* 223:162–173
- Erto A, Andreozzi R, Natale FD, Lancia A, Musmarra D (2010) Experimental and statistical analysis of trichloroethylene adsorption onto activated carbon. *Chem Eng J* 156:353–359
- Hameed BH, El-Khaiary MI (2008) Sorption kinetics and isotherm studies of a cationic dye using agricultural waste: broad bean peels. *J Hazard Mater* 154:639–648
- Ho YS, Ofomaja AE (2006) Pseudo-second-order model for lead ion sorption from aqueous solutions onto palm kernel fiber. *J Hazard Mater B* 129:137–142
- Ioannou Z, Simitzis J (2009) Adsorption kinetics of phenol and 3-nitrophenol from aqueous solutions on conventional and novel carbons. *J Hazard Mater* 171:954–964
- Jo YJ, Lee JY, Yi MJ, Kim HS, Lee KK (2010) Soil contamination with TCE in an industrial complex: contamination levels and implication for groundwater contamination. *Geosci J* 14:313–320
- Kannan N, Sundaram MM (2001) Kinetics and mechanism of removal of methylene blue by adsorption on various carbons – a comparative study. *Dyes Pigments* 51:25–40
- Karanfil T, Dastgheib SA (2004) Trichloroethylene adsorption by fibrous and granular activated carbons: aqueous phase, gas phase, and water vapor adsorption studies. *Environ Sci Technol* 38:5834–5841
- Keiluweit M, Nico PS, Johnson MG, Kleber M (2010) Dynamic molecular structure of plant biomass-derived black carbon (Biochar). *Environ Sci Technol* 44:1247–1253
- Kim J, Kim M, Hyun S, Kim JG, Ok YS (2012) Sorption of acidic organic solute onto kaolinitic soils from methanol-water mixture. *J Environ Sci Health Part B* 47:22–29
- Klasson KT, Wartelle LH, Lima IM, Marshall WE, Akin DE (2009) Activated carbons from flax shive and cotton gin waste as environmental adsorbents for the chlorinated hydrocarbon trichloroethylene. *Bioresour Technol* 100:5045–5050
- Kumar KV, Porkodi K, Rocha F (2008) Comparison of various error functions in predicting the optimum isotherm by linear and non-

- linear regression analysis for the sorption of basic red 9 by activated carbon. *J Hazard Mater* 150:158–165
- Leboda R, Lodyga A, Gierak A (1997) Carbon adsorbents as materials for chromatography I. Gas chromatography. *Mater Chem Phys* 51:216–232
- Lee JY, Lee KK (2004) A short note on investigation and remediation of contaminated groundwater and soil in Korea. *J Eng Geol* 14:123–130
- Lee JW, Kidder M, Evans BR, Paik S, Buchanan AC III, Garten CT, Brown RC (2010) Characterization of biochars produced from cornstovers for soil amendments. *Environ Sci Technol* 44:7970–7974
- Lee SS, Lim JE, El-Azeem SAMA, Choi B, Oh SE, Moon DH, Ok YS (2013) Heavy metal immobilization in soil near abandoned mines using eggshell waste and rapeseed residue. *Environ Sci Pollut Res* 20:1719–1726
- Li L, Quinlivan PA, Knappe DRU (2002) Effects of activated carbon surface chemistry and pore structure on the adsorption of organic contaminants from aqueous solution. *Carbon* 40:2085–2100
- Mohammad SAS, Maya N (2011) A review and evaluation of selected kinetic models and sorption processes in amended soils. *Int J Res Chem Environ* 1:1–14
- Novak JM, Lima I, Xing B, Gaskin JW, Steiner C, Das KC, Ahmedna M, Rehrh D, Watts DW, Busscher WJ, Schomberg H (2009) Characterization of designer biochar produced at different temperatures and their effects on a loamy sand. *Ann Environ Sci* 3:195–206
- Ok YS, Yang JE, Zhang YS, Kim SJ, Chung DY (2007) Heavy metal adsorption by a formulated zeolite-Portland cement mixture. *J Hazard Mater* 147:91–96
- Ok YS, Oh SE, Ahmad M, Hyun S, Kim KR, Moon DH, Lee SS, Lim KJ, Jeon WT, Yang JE (2010) Effects of natural and calcined oyster shells on Cd and Pb immobilization in contaminated soils. *Environ Earth Sci* 61:1301–1308
- Ok YS, Usman ARA, Lee SS, Abd El-Azeem SAM, Choi B, Hashimoto Y, Yang JE (2011) Effects of rapeseed residue on lead and cadmium availability and uptake by rice plants in heavy metal contaminated paddy soil. *Chemosphere* 85:677–682
- Park M, Komarneni S (1998) Stepwise functionalization of mesoporous crystalline silica materials. *Micropor Mesopor Mater* 25:75–80
- Park JH, Lamb D, Paneerselvam P, Choppala G, Bolan N, Chung JW (2011) Role of organic amendments on enhanced bioremediation of heavy metal(loid) contaminated soils. *J Hazard Mater* 185:549–574
- Pellera FM, Giannis A, Kalderis D, Anastasiadou K, Stegmann R, Wang JY, Gidarakos E (2012) Adsorption of Cu(II) ions from aqueous solutions on biochars prepared from agricultural by-products. *J Environ Manag* 96:35–42
- Plazinski W, Rudzinski W, Palzinska A (2009) Theoretical models of sorption kinetics including a reaction mechanism: a review. *Adv Colloid Interface Sci* 152:2–13
- Qui Y, Zheng Z, Zhou Z, Sheng DG (2009) Effectiveness and mechanisms of dye adsorption on a straw-based biochar. *Bioresour Technol* 100:5348–5351
- Quinlivan PA, Li L, Knappe DRU (2005) Effects of activated carbon characteristics on the simultaneous adsorption of aqueous organic micropollutants and natural organic matter. *Water Res* 39:1663–1673
- Saeed A, Akhter MW, Iqbal M (2005) Removal and recovery of heavy metals from aqueous solution using papaya wood as a new biosorbent. *Sep Purif Technol* 45:25–31
- Salih HH, Patterson CL, Sorial GA, Sinha R, Krishnan R (2011) The fate and transport of the SiO₂ nanoparticles in a granular activated carbon bed and their impact on the removal of VOCs. *J Hazard Mater* 193:95–101
- Spokas KA, Novak JM, Stewart CE, Cantrell KB, Uchimiya M, DuSaire MG, Ro KS (2011) Qualitative analysis of volatile organic compounds on biochars. *Chemosphere* 85:869–882
- Uchimiya M, Wartelle LH, Lima IM, Klasson KT (2010) Sorption of deisopropylatrazine on broiler litter biochars. *J Agric Food Chem* 58:12350–12356
- Wei Z, Seo Y (2010) Trichloroethylene (TCE) adsorption using sustainable organic mulch. *J Hazard Mater* 181:147–153
- Witek-Krowiak A, Szafran RG, Modelski S (2011) Biosorption of heavy metals from aqueous solutions onto peanut shell as a low cost biosorbent. *Desalination* 265:126–134
- Wong YC, Szeto YS, Cheung WH, McKay G (2004) Pseudo-first-order kinetic studies of the sorption of acid dyes onto chitosan. *J Appl Polym Sci* 92:1633–1645
- Xu X, Cao X, Zhao L, Wang H, Yu H, Gao B (2012) Removal of Cu, Zn, and Cd from aqueous solutions by the dairy manure-derived biochar. *Environ Sci Pollut Res*. doi:10.1007/s11356-012-0873-5
- Yang JE, Kim JS, Ok YS, Kim SJ, Yoo KY (2006) Capacity of Cr(VI) reduction in an aqueous solution using different sources of zerovalent irons. *Korean J Chem Eng* 23:935–939
- Yang JE, Kim JS, Ok YS, Yoo KR (2007) Mechanistic evidence and efficiency of the Cr(VI) reduction in water by different sources of zerovalent irons. *Water Sci Technol* 55:197–202
- Yang JE, Skogley EO, Ok YS (2011) Carbonaceous resin capsule for vapor-phase monitoring of volatile monoaromatic hydrocarbons in soil. *Soil Sediment Contam* 20:205–220
- Yu SY, Chae GT, Jeon KH, Jeong JS, Park JG (2006) Trichloroethylene contamination in fractured bedrock aquifer in Wonju, South Korea. *Bull Environ Contam Toxicol* 76:341–348
- Yu X, Pan L, Ying G, Kookana RS (2010) Enhanced and irreversible sorption of pesticide pyrimethanil by soil amended with biochars. *J Environ Sci* 22:615–620
- Zhang P, Sun H, Yu L, Sun T (2013) Adsorption and catalytic hydrolysis of carbaryl and atrazine on pig manure-derived biochars: impacts of structural properties of biochars. *J Hazard Mater* 244–245:217–224